Journal of Fluorine Chemistry 130 (2009) 1059–1062

Contents lists available at ScienceDirect

Journal of Fluorine Chemistry

journal homepage: www.elsevier.com/locate/fluor

Short communication

Effect of crystal structure and ions concentration on luminescence in Yb^{3+} and Tm^{3+} codoped fluoride microcrystals

Lili Wang [a,b], Chunyan Cao [c], Xiaojie Xue [a], Dan Zhao [a], Daisheng Zhang [a], Kezhi Zheng [a], Ning Liu [a], Feng Shi [a], Chunfeng He [a], Weiping Qin [a,*]

[a] State Key Laboratory on Integrated Optoelectronics, College of Electronic Science and Engineering, Jilin University, Changchun 130012, China
[b] School of Basic Sciences, Changchun University of Technology, Changchun 130012, China
[c] College of Mathematics and Physics, Jinggangshan University, Jian 343009, China

ARTICLE INFO

Article history:
Received 23 July 2009
Received in revised form 18 August 2009
Accepted 1 September 2009
Available online 6 September 2009

Keywords:
Upconversion
Rare-earth
Fluoride

ABSTRACT

A facile hydrothermal method is used for the preparation of Tm^{3+}/Yb^{3+} codoped fluoride microphosphors. The effect of crystal structure and ions concentration on the spectra and lifetimes of the radiative levels of Tm^{3+} ions in the different fluoride microcrystals is studied in detail. XRD analysis of Tm^{3+}/Yb^{3+} codoped LaF_3 microcrystals shows that 20% Yb^{3+} doping is sufficient for hexagonal LaF_3 microparticles to crystallize completely in the orthorhombic phase. And lifetime analysis suggests that the average lifetimes of the radiative levels of Tm^{3+} ions increased when the matrix phase structure changing from orthorhombic phase to hexagonal phase with ytterbium dopant concentration changing.

1. Introduction

Infrared-to-visible frequency upconversion in lanthanide-doped materials has been extensively investigated owing to their potential applications in visible upconversion lasers, high density memories, and solid-state color displays [1]. Thus, there exists a need for alternative solid-state color materials capable of producing efficient frequency upconversion luminescence. The fluoride matrix seems to be an ideal medium for the preparation of efficient upconversion luminescent materials, because of their lower phonon energy compared with oxide hosts. Over the past few years, a great deal of attention has been paid on rare-earth doped fluoride microcrystals (MCs) and several groups have already demonstrated efficient upconversion luminescence properties of rare-earth doped fluoride crystals [2–4]. However, from the fundamental point of view, above potential applications are still reliant on the crystal phase design. So the studying on the luminescence properties of rare-earth ions in different fluoride microcrystals with various crystal phase, as well as local structure is very important. Further fundamental research in this field remains a challenge.

In case of rare-earth ions, the electronic f–f transitions involve electrons which are localized in atomic orbitals of the ions. Therefore, no size-dependent quantization effect (due to confinement of delocalized electrons) is found in these transitions. However, confinement effects may be induced by inter-ionic electronic interaction and electron–phonon interaction. Particularly, the electron–phonon interaction has strong influence on the luminescence properties. Some references have reported that the upconversion luminescence spectra were sensitive to the crystal structure and dopant concentration [5,6]. However, phase change of these samples depends upon increasing the calcined temperature, as well as changing experimental conditions. As we know, except for crystal structure, experimental conditions also determine the features of fluorescence spectroscopy for a given optically active ion [7–10]. So when we investigated spectra feature, experimental conditions as a factor cannot be ignored. Under the same experimental condition, no report has been found on the effect of crystal structure upon the spectra of Tm^{3+} ions in different fluoride microcrystals, to our knowledge. Furthermore, when the LaF_3 and YF_3 are prepared under the same conditions, they are similar in size. It is known that the main crystal phases of LaF_3 are hexagonal, YbF_3 and YF_3 are orthorhombic. In this letter, we study the effect of ytterbium dopant on the crystal structure of microparticles and show the influences of crystal structure as well as ytterbium dopant concentration on the luminescence properties of Tm^{3+} ions in different fluoride host prepared under the same condition.

---

[*] Corresponding author. Tel.: +86 431 85168241/8325; fax: +86 431 85168241/8325.
E-mail address: wpqin@jlu.edu.cn (W. Qin).

0022-1139/$ – see front matter © 2009 Elsevier B.V. All rights reserved.
doi:10.1016/j.jfluchem.2009.09.001

2. Results and discussion

2.1. Crystal structure and morphology

To check the phase purity and phase structure, X-ray diffraction (XRD) measurements were carried out for a series of powder samples, as shown in Fig. 1. The annealed samples LaF_3:10Yb^{3+}, 0.5Tm^{3+} MCs in Fig. 1(a) is in well agreement with that of the standard hexagonal LaF_3 (JCPDS: 72-1435) with the same space group P6322 (182). However with the concentration of the Yb^{3+} ions increased to 20% the crystal phase of the annealed sample LaF_3:20Yb^{3+}, 0.5Tm^{3+} MCs in Fig. 1(a) is in well agreement with that of the orthorhombic YbF_3 (JCPDS: 74-2178) with the same space group Pnma (62). There is no phase impurity in these samples. These results indicate that 20% Yb^{3+} doping is sufficient for hexagonal LaF_3 microparticles to crystallize completely in the orthorhombic phase. The annealed sample YF_3:10Yb^{3+}, 0.5Tm^{3+} MCs in Fig. 1(b) is in well agreement with that of the orthorhombic YF_3 (JCPDS: 74-0911) with the same space group Pnma (62). It is known that orthorhombic phase is less symmetric than hexagonal phase. The dependence of luminescence on the local environment can be obtained by comparing the spectra of these three samples. The inset in Fig. 1 shows the SEM images of the corresponding samples. They clearly show that these samples were composed of aggregated particles and were similar in size.

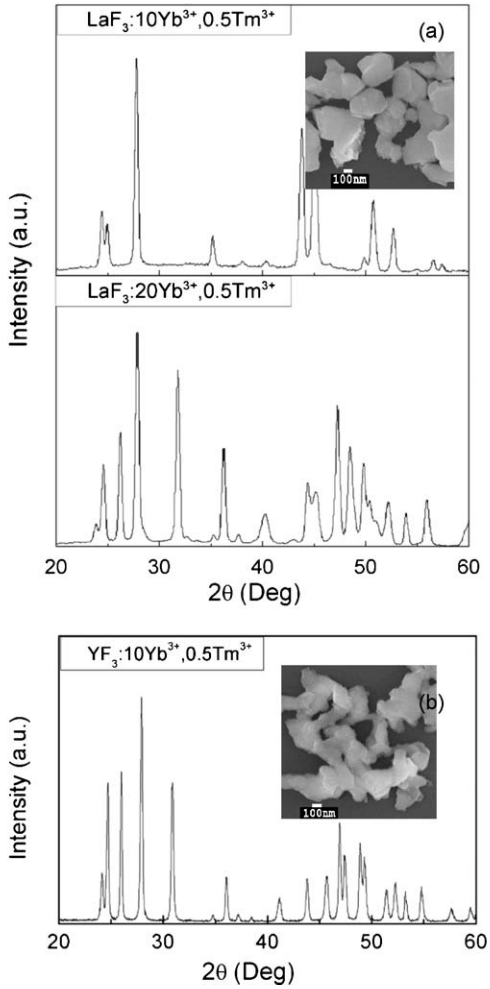

Fig. 1. XRD patterns of samples (a) LaF_3:10Yb^{3+}, 0.5Tm^{3+}; LaF_3:20Yb^{3+}, 0.5Tm^{3+}; (b) YF_3:10Yb^{3+}, 0.5Tm^{3+} MCs annealed at 600 °C.

2.2. Luminescence characteristics

Fig. 2 depicts the emission spectra of Tm^{3+} ions doped in LaF_3 and YF_3 MCs at different concentrations. The spectra were all recorded under the same conditions (emission slit is 1.0 nm, high voltage of the photomultiplier tube is 400 V, scan speed is 240 nm/min and the excitation power density is about 60 W/cm^2). The emission peak around 360 nm is due to $^1D_2 \rightarrow {}^3H_6$ transition of Tm^{3+} ions (Fig. 2(a)), and that around 474 nm is due to $^1G_4 \rightarrow {}^3H_6$ transition of Tm^{3+} ions (Fig. 2(b)). Generally, the f–f transition is very narrow and exhibit multiple structures derived from electronic interactions, as well as spin–orbit coupling. These distinct peaks (denoted as Δ) are due to the Stark splitting of the $^3H_6$ level of Tm^{3+} ions in LaF_3:20Yb^{3+}, 0.5Tm^{3+} and YF_3:10Yb^{3+}, 0.5Tm^{3+} MCs. The Stark splitting is caused by the crystal fields [6] and can be discern more clearly from the broader peaks of room temperature under low temperatures. In this paper, we study the Stark splitting of Tm^{3+} ions at room temperature. The corresponding emissions of the Tm^{3+} ions in LaF_3:10Yb^{3+}, 0.5Tm^{3+} only exhibit broadened feature and unconspicuous Stark splitting. According to the literature, lower number of Stark levels just represents a higher symmetry of Tm^{3+} ions in hexagonal LaF_3:10Yb^{3+}, 0.5Tm^{3+} microparticles compared with that in orthorhombic LaF_3:20Yb^{3+}, 0.5Tm^{3+} and YF_3:10Yb^{3+}, 0.5Tm^{3+} MCs [5,6]. Its relatively higher symmetry in hexagonal LaF_3:10Yb^{3+}, 0.5Tm^{3+} is not enough to create distinct splitting. The spectra of higher concentration of Yb^{3+} ions (20 mol%) in LaF_3 matrix show higher number of distinct splitting than that of 10 mol% Yb^{3+} in LaF_3 matrix, because 20% Yb^{3+} ions doping is sufficient for hexagonal LaF_3 MCs to crystallize completely in the orthorhombic phase. This clearly indicates that the crystal structure, as well as ytterbium dopant concentration has strong affect on luminescence of Tm^{3+} ions in LaF_3 MCs. To eliminate the influence of energy transfer, when improving concentration of Yb^{3+} ions, we also prepare the sample of orthorhombic YF_3:10Yb^{3+}, 0.5Tm^{3+} MCs. Its spectrum (Fig. 2) is still different from 10 mol% Yb^{3+} containing LaF_3 MCs, due to the different crystal structure and symmetry between them.

Observation of fluorescence temporal decay is another effective way to investigate the change in the local environment, because the decay time can be affected significantly by the local environment [7]. The temporal evolution of Tm^{3+} luminescence in the microcrystals was studied and the time-dependent emission profile for the representative emission (347.2 nm) from $^1I_6$ level of Tm^{3+} ions was recorded, as shown in Fig. 3. This decay curve can be fitted well into a single-exponential function as $I = I_0\exp(-t/\tau)$ (I_0 is the initial emission intensity at $t = 0$ and τ is the lifetime of the emission center). The inverse of τ is equal to the sum of the spontaneous (radiative) emission rate and nonradiative relaxation rate. Herein, the nonradiative relaxation rate should be of the same order of magnitude because our three samples are prepared under the same conditions. According to the best-fitted result, the lifetimes of the other emission levels of Tm^{3+} ions and that of other samples are listed in Table 1. As can be seen from Table 1, the results suggest that the decay times increased when the phase structure changing from orthorhombic phase to hexagonal phase. That is because the transition probability of Tm^{3+} ions in orthorhombic LaF_3:20Yb^{3+}, 0.5Tm^{3+} and YF_3:10Yb^{3+}, 0.5Tm^{3+} MCs increased due to the low site symmetry of their crystals. It should be remembered that the f–f transitions arising from forced electric dipole transitions which are parity forbidden and become partially allowed when the ion is situated at low symmetry site. Such situation allows intermixing of the f states with higher electronic configuration [11] and as a result the radiative emission rate increases, i.e. the lifetime decreases when ignoring the influence of nonradiative relaxation rate. In the case of higher

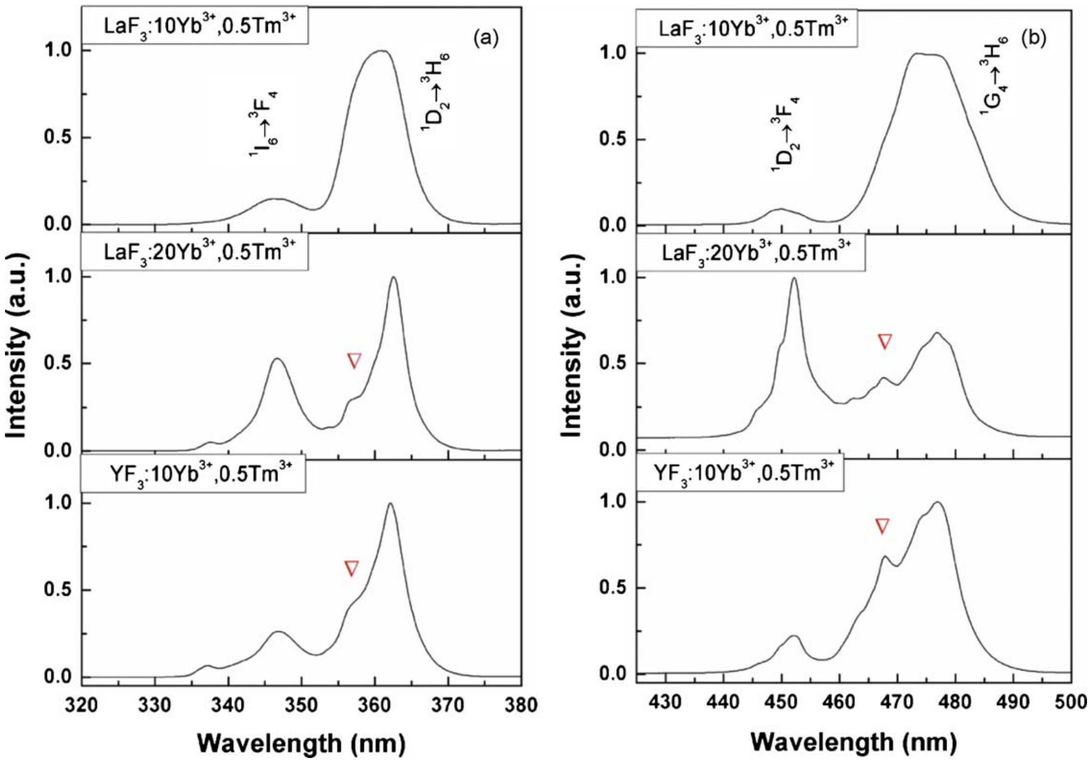

Fig. 2. Upconversion emission spectra of Tm^{3+} ions under 980 nm excitation in LaF_3:$10Yb^{3+}$, $0.5Tm^{3+}$; LaF_3:$20Yb^{3+}$, $0.5Tm^{3+}$; YF_3:$10Yb^{3+}$, $0.5Tm^{3+}$ MCs.

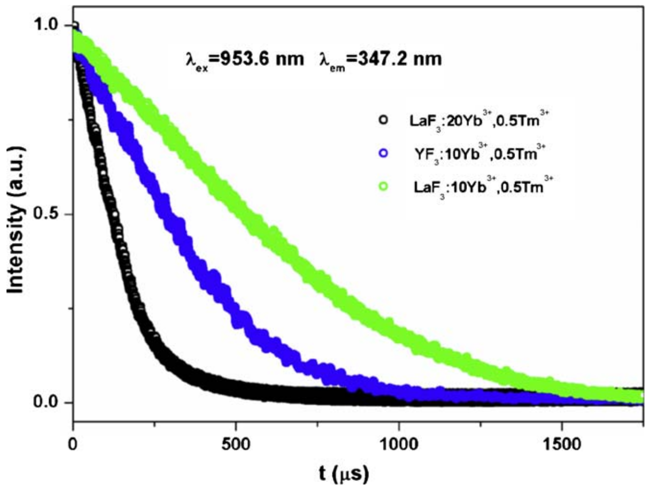

Fig. 3. Decay curve of 347.2 nm emission under 953.6 nm excitation in LaF_3:$10Yb^{3+}$, $0.5Tm^{3+}$; LaF_3:$20Yb^{3+}$, $0.5Tm^{3+}$; YF_3:$10Yb^{3+}$, $0.5Tm^{3+}$ MCs.

Table 1
Decay times of $^1I_6$, $^1D_2$ and $^1G_4$ levels of Tm^{3+} ions in LaF_3:$10Yb^{3+}$, $0.5Tm^{3+}$; LaF_3:$20Yb^{3+}$, $0.5Tm^{3+}$ and YF_3:$10Yb^{3+}$, $0.5Tm^{3+}$ MCs calculated from the decay curves analysis.

Sample	$^1I_6$ (μs)	$^1D_2$ (μs)	$^1G_4$ (μs)
LaF_3:$10Yb^{3+}$, $0.5Tm^{3+}$ (hexagonal)	512	671	3832
YF_3:$10Yb^{3+}$, $0.5Tm^{3+}$ (orthorhombic)	288	390	1758
LaF_3:$20Yb^{3+}$, $0.5Tm^{3+}$ (orthorhombic)	138	152	400

concentration of Yb^{3+} ions in LaF_3:$20Yb^{3+}$, $0.5Tm^{3+}$ MCs, this asymmetric environment is one of the lifetime decreasing reasons. And the other reason is energy back transfer from Tm^{3+} ions to Yb^{3+} ions due to the high concentration of Yb^{3+} ions in the crystals. These two reasons induced the decay time decreased dramatically. Analysis suggests that crystal phase and dopant concentration affect decay time of the radiative levels of Tm^{3+} ions doped in fluoride microcrystals.

3. Conclusion

In conclusion, Tm^{3+}/Yb^{3+} codoped LaF_3 and YF_3 MCs were prepared according to the same procedure. 20% Yb^{3+} ions doping makes the hexagonal LaF_3 crystallizing completely in orthorhombic phase. Dopant concentration and crystal structure have obvious effect on the luminescence spectra of Tm^{3+} ions and lifetimes of the radiative levels of Tm^{3+} ions. Therefore, an asymmetric crystal host and judicious choice of dopant concentration are responsible for efficient emission of Tm^{3+} ions in fluoride MCs.

4. Experimental details

Tm^{3+}/Yb^{3+} codoped LnF_3 (Ln = Y, La) MCs were synthesized using a simple hydrothermal method [12]. The MCs were prepared from Y_2O_3 (Aldrich), La_2O_3 (Aldrich), Tm_2O_3 (Aldrich), and Yb_2O_3 (Aldrich) according to the following compositions in molar fraction: $(0.995 - x)$ Ln_2O_3–0.005 Tm_2O_3–xYb_2O_3 ($x = 0.10, 0.20$) (Ln = Y, La). The RE oxides were dissolved in nitric acid (Aldrich 63%) to form a clear solution, and then the hydrofluoric acid (Aldrich 40%) was added dropwise. After being vigorously stirred for 30 min, the suspension solution was transferred to a 50 mL stainless Teflon-lined autoclave and heated at 130 °C for 12 h. After being cooled to room temperature naturally, the upper clear solution was discarded, and the remainder was washed several times with deionized water. The resultant material was dried in a vacuum at 60 °C for several hours, and white powder samples were obtained. After being annealed under an Ar atmosphere at 600 °C for 1 h, these samples emitted bright blue light under 980 nm excitation. To identify the crystallization phase, X-ray-diffraction (XRD) analysis was carried out with a powder diffractometer (Model Rigaku RU-200b), using Ni-filtered Cu Kα radiation (λ = 1.5406 Å). The size and the morphology of the samples were further examined using a scanning electron microscopy (JEOL JSM-7500F). Upconversion emission spectra of the samples were recorded with a fluorescence spectrophotometer (Hitachi F-4500). A power-adjustable laser diode (980 nm, 0–2 W) with a lens making the beam parallel was employed as the upconversion excitation source. A YAG:Nd pulsed laser (duration of 10 ns and maximum energy of 0.6 J per pulse with a second harmonic generator) was used to pump a Raman shifter. The Raman shifter was filled with high-purity hydrogen at 300 psi. Through an optical dispersing prism and a filter (gallium–arsenide slice), a second Stokes excited Raman laser at 953.6 nm was used as the pulsed excitation source for our measurements of fluorescent lifetimes. All measurements were performed at room temperature.

Acknowledgements

This work was supported by the National High Technology Research and Development Program of China (863 Program) and the National Natural Science Foundation of China (NNSFC) (grant nos. 10874058 and 50672030).

References

[1] F. Auzel, Chem. Rev. 104 (2004) 139–174.
[2] Y. Wang, W. Qin, J. Zhang, C. Cao, J. Zhang, Y. Jin, P. Zhu, G. Wei, G. Wang, L. Wang, Chem. Lett. 36 (2007) 912–913.
[3] G.F. Wang, W.P. Qin, J.S. Zhang, L.L. Wang, G.D. Wei, P.F. Zhu, R. Kim, J. Alloy. Compd. 475 (2009) 452–455.
[4] G.F. Wang, W.P. Qin, L.L. Wang, G.D. Wei, P.F. Zhu, R.J. Kim, Opt. Exp. 16 (2008) 11907–11914.
[5] P. Amitava, S.F. Christopher, K. Rakesh, N.P. Paras, Appl. Phys. Lett. 83 (2003) 284–286.
[6] A. Patra, Chem. Phys. Lett. 387 (2004) 35–39.
[7] H.R. Zheng, X.J. Wang, S.X. Qu, M.J. Dejneka, R.S. Meltzer, J. Lumin. 119 (2006) 153–160.
[8] R.S. Meltzer, S.P. Feofilov, B. Tissue, H.B. Yuan, Phys. Rev. B 60 (1999) R14012–R14015.
[9] H. Peng, S. Huang, L. Sun, C. Yan, Phys. Lett. A 367 (2007) 211–214.
[10] G. Ozen, O. Forte, B. Di Bartolo, J.M. Collins, J. Appl. Phys. 102 (2007) 023110.
[11] A. Patra, E. Sominska, S. Ramesh, Y. Koltypin, Z. Zhong, H. Minti, R. Reisfeld, A. Gedanken, J. Phys. Chem. B 103 (1999) 3361–3365.
[12] W.P. Qin, C.Y. Cao, L.L. Wang, J.S. Zhang, D.S. Zhang, K.Z. Zheng, Y. Wang, G.D. Wei, G.F. Wang, P.F. Zhu, R. Kim, Opt. Lett. 33 (2008) 2167–2169.